

Dalton Transactions

Accepted Manuscript



This is an *Accepted Manuscript*, which has been through the Royal Society of Chemistry peer review process and has been accepted for publication.

Accepted Manuscripts are published online shortly after acceptance, before technical editing, formatting and proof reading. Using this free service, authors can make their results available to the community, in citable form, before we publish the edited article. We will replace this *Accepted Manuscript* with the edited and formatted *Advance Article* as soon as it is available.

You can find more information about *Accepted Manuscripts* in the [Information for Authors](#).

Please note that technical editing may introduce minor changes to the text and/or graphics, which may alter content. The journal's standard [Terms & Conditions](#) and the [Ethical guidelines](#) still apply. In no event shall the Royal Society of Chemistry be held responsible for any errors or omissions in this *Accepted Manuscript* or any consequences arising from the use of any information it contains.

Antiferromagnetic Cu-Gd interactions through oxime bridge

Jean-Pierre Costes,^{a,b*}, Carine Duhayon,^{a,b} Sonia Mallet-Ladeira,^{a,b} Laure Vendier,^{a,b} Javier

Garcia-Tojal,^{a,c} Luisa Lopez Banet^{a,d}

^a *Laboratoire de Chimie de Coordination du CNRS, 205, route de Narbonne, BP 44099, F-31077 Toulouse Cedex 4, France*

^b *Université de Toulouse ; UPS, INPT, F-31077 Toulouse Cedex 4, France*

^c *Universidad de Burgos, Facultad de Ciencias, Departamento de Química, Plaza Misae Banuelos, s/n 09001 Burgos, Spain*

^d *Universidad de Murcia, Departamento de Química Inorganica, E-30071 Murcia, Spain*

Abstract. The copper complex of a polydentate non symmetrical Schiff base ligand [LCu]₂, prepared by template synthesis, has been reacted with the series of Lanthanide ions. This complex used as ligand possesses two functions (phenol and oxime) able to coordinate the Ln ions and, according to the Ln ion, three types of complexes are obtained. From La to Eu, trinuclear [(LCu)₂Ln(NO₃)₃] complexes with a double phenoxo-oximato bridge are isolated. From Gd to Ho, the complexes [(LCu)₂Ln(NO₃)₃(H₂O)] are still trinuclear, with a supplementary water molecule linked to the Ln ion but the Cu^{II} and Ln^{III} ions are only bridged by the oximato (N-O) pair, the phenoxo oxygen atom being hydrogen-bridged to the Ln-coordinated water molecule. Then with heavier Ln ions, dinuclear [(LCu)Ln(NO₃)₃(H₂O)₂] complexes are characterized. The magnetic study demonstrates that the oximato bridge is responsible for the antiferromagnetic character of the Cu-Gd interaction, with $J_{CuGd} = -0.63$ cm⁻¹ in [(LCu)₂Gd(NO₃)₃(H₂O)], in contrast to the ferromagnetic Cu-Gd interaction induced by the single oxygen atom phenoxo bridge.

Keywords: 3d-Gd complexes, Structural determinations, Oximato bridge, Antiferromagnetic Cu-Gd interaction.

Introduction

A lot of strictly heterodinuclear 3d-4f complexes have been prepared in the last twenty years,¹⁻⁴ and the magnetic studies of the complexes assembling copper or nickel ions with the isotropic gadolinium ions Gd^{III} do confirm presence of ferromagnetic Cu-Gd or Ni-Gd interactions in the huge majority of cases. The largest magnetic interactions are observed with the complexes involving a double phenoxo bridge,⁵⁻⁶ the strength of the magnetic interaction being related to the hinge angle, which is defined as the dihedral angle between the O-Cu-O or O-Ni-O and O-Gd-O planes forming the bridging unit. Indeed planar Cu(μ -O₂)Gd and Ni(μ -O₂)Gd bridging fragments give the largest magnetic interactions. And it has been shown that large Ni-O-Gd bridging angles, defined as θ , are associated with the larger Ni-Gd interactions.⁷ When the Co^{II} ions are concerned, it has been recently shown that ferromagnetic interactions are again observed with high spin Co^{II} ions characterized by singly-occupied σ d_{x²-y²} orbital ($S = 3/2$) while these interactions become antiferromagnetic with low spin Co^{II} ions ($S = 1/2$) having unoccupied σ d_{x²-y²} orbital.⁸ All these observations, cobalt complexes, hinge and bridging angles, are in agreement with a preponderant role played by the d_{x²-y²} orbitals. A look at the examples yielding antiferromagnetic Cu-Gd interactions highlights presence of one or two oxime functions bridging the metal ions.⁹⁻¹³ Contrary to the phenoxo bridge involving a unique oxygen atom in between the metal ions, two atoms, a nitrogen and an oxygen atoms, are implied in that bridge. But the discrete Gd₄Cu¹⁰ or the polymeric [Gd₂Cu₂]_n chains¹³ involving dioxime bridges are not easy to study from the magnetic point of view, due to the concomitant presence of Cu-Gd and Gd-Gd interactions. In the other compounds dominated by antiferromagnetic interactions, the simultaneous participation of two different functions to the bridge, a monoatomic phenoxo and a diatomic oxime function,¹¹⁻¹² does not allow to determine the participation of each function to the overall magnetic interaction. In order to better understand the magnetic interaction through the N-O diatomic oxime bridge, we have designed a LCu complex prepared thanks to the template effect of the Cu^{II} ions, that can react as a ligand toward Ln ions through its phenoxo and oximato functions. Previous structural determinations have shown that with Cerium, an early Ln ion with a large ionic radius, a trinuclear [(LCu)₂Ce(NO₃)₃] complex¹² with a double phenoxo-oximato bridge is obtained while reaction with late Er or Yb ions yields dinuclear LCuLn(NO₃)₃(H₂O)₂(C₃H₆O)] complexes with a single oximato bridge between the Cu and Ln ions.¹⁴ Due to the lack of structural characterizations, the situation for the ions positioned in the middle of the Ln series is not known. This is why we decided to complete the series of

complexes in order to better understand what happens all along the series. We describe here the structural determination of the [(LCu)₂Tb(NO₃)₃(H₂O)] entity and confirm by X-Ray powder diffraction that the equivalent [(LCu)₂Gd(NO₃)₃(H₂O)] compound is isostructural. These experimental results combined to recently published theoretical data¹⁵ give an interesting information on the general M-oximate-Gd magnetic interaction.

Experimental Section

Materials.

Salicylaldehyde, hexafluoroacetylacetone (Hhfa), Cu(OAc)₂·2H₂O, Gd(NO₃)₃·6H₂O, Tb(NO₃)₃·6H₂O (Aldrich) were used as purchased. Gd(hfa)₃·2H₂O,¹⁶ (hfa = hexafluoroacetylacetonate), Gd(hfa)₂(Hhfa)(CH₃CO₂)¹⁷ and Cu(Sal)₂¹⁸ (Sal = salicylaldehyde) were prepared as previously described. High-grade solvents (diethyl ether, pentane, dimethylformamide, acetone and methanol) were used for the syntheses of ligands and complexes.

Complexes.

[LCu]₂. 1 This complex was prepared as previously described.^{12,14} Recrystallization from hot dimethylformamide yielded crystals suitable for X-Ray diffraction study.

As the reaction process with diverse Ln ions is similar, we only describe the preparation of the Lanthanum complex, followed by the analytical results and infrared data for the entire series of complexes.

[(LCu)₂La(NO₃)₃]. 2 A mixture of LCu (0.17 g, 5 × 10⁻⁴ mol) and La(NO₃)₃·5H₂O (0.21 g, 5 × 10⁻⁴ mol) in acetone (10 mL) was heated for ten minutes and then left to cool with stirring, thus yielding a precipitate that was filtered off and dried. Yield : 0.17 g (65 %). Anal. Calcd for C₃₀H₃₈Cu₂LaN₉O₁₃: (998.7) C, 36.1; H, 3.8; N, 12.6. Found : C, 35.6; H, 3.7; N, 12.2. IR (ATR): 2974w, 1630s, 1603m, 1547w, 1485m, 1475m, 1438s, 1431s, 1396m, 1369w, 1303s, 1285s, 1224m, 1186w, 1162w, 1130s, 1027w, 911w, 886w, 816w, 769m, 756m, 728w, 690w cm⁻¹.

[(LCu)₂Ce(NO₃)₃]. 3¹² Yield : 0.18 g (70 %). Anal. Calcd for C₃₀H₃₈CeCu₂N₉O₁₃: (1000.0) C, 36.0; H, 3.8; N, 12.6. Found : C, 35.6; H, 3.4; N, 12.3. IR (ATR): 2974w, 1630s, 1603m, 1546w, 1486m, 1474m, 1438s, 1431s, 1396m, 1369w, 1303s, 1284s, 1224m, 1186w, 1162w, 1130s, 1027w, 911w, 886w, 816w, 769m, 755m, 729w, 690w cm⁻¹.

[(LCu)₂Pr(NO₃)₃]. 4 Yield : 0.17 g (70 %). Anal. Calcd for C₃₀H₃₈Cu₂N₉O₁₃Pr: (1000.7) C, 36.0; H, 3.8; N, 12.6. Found : C, 35.5; H, 3.5; N, 12.1. IR (ATR): 2974w, 1630s, 1603m, 1546w, 1486m, 1474m, 1439s, 1431s, 1396m, 1369w, 1304s, 1285s, 1224m, 1186w, 1162w, 1130s, 1028w, 911w, 886w, 816w, 769m, 755m, 731w, 690w cm⁻¹.

[(LCu)₂Nd(NO₃)₃].5 Yield : 0.17 g (68 %). Anal. Calcd for C₃₀H₃₈Cu₂N₉O₁₃Nd (1004.0) C, 35.9; H, 3.8; N, 12.6. Found : C, 35.6; H, 3.6; N, 12.02. IR (ATR): 2974w, 1631s, 1604m, 1546w, 1488m, 1474m, 1439s, 1396m, 1369w, 1312s, 1285s, 1279s, 1225m, 1186w, 1163w, 1130s, 1028w, 911w, 885w, 815w, 769m, 755m, 732w, 690w cm⁻¹.

[(LCu)₂Sm(NO₃)₃]. 6 Yield : 0.16 g (64 %). Anal. Calcd for C₃₀H₃₈Cu₂N₉O₁₃Sm (1010.1) C, 35.7; H, 3.8; N, 12.5. Found : C, 35.5; H, 3.4; N, 12.0. IR (ATR): 2974w, 1631s, 1604m, 1546w, 1488m, 1474m, 1440s, 1396m, 1369w, 1308s, 1279s, 1229m, 1186w, 1163w, 1130s, 1028w, 910w, 885w, 815w, 768m, 755m, 733w, 690w cm⁻¹.

[(LCu)₂Eu(NO₃)₃]. 7 Yield : 0.15 g (60 %). Anal. Calcd for C₃₀H₃₈Cu₂EuN₉O₁₃ (1011.7) C, 35.6; H, 3.8; N, 12.5. Found : C, 35.2; H, 3.6; N, 12.1. IR (ATR): 2974w, 1631s, 1604m, 1545w, 1489m, 1474m, 1441s, 1396m, 1369w, 1309s, 1280s, 1229m, 1186w, 1163w, 1130s, 1028w, 912w, 886w, 815w, 768m, 755m, 733w, 690w cm⁻¹.

[(LCu)₂Gd(NO₃)₃(H₂O)]. 8 Yield : (85 %). Anal. Calcd for C₃₀H₄₀Cu₂GdN₉O₁₄: (1035.0) C, 34.8; H, 3.9; N, 12.2. Found : C, 34.4; H, 3.6; N, 11.9. IR (ATR): 3097l, 2966w, 1629s, 1604m, 1543w, 1476s, 1445s, 1299m, 1287s, 1225m, 1191w, 1154w, 1128s, 1026w, 915w, 816w, 766m, 743w, 695w cm⁻¹.

[(LCu)₂Tb(NO₃)₃(H₂O)]. 9 Slow evaporation of the filtrate yielded crystals suitable for XRD. Yield : 0.17 g (65 %). Anal. Calcd for C₃₀H₄₀Cu₂N₉O₁₄Tb: (1036.7) C, 34.8; H, 3.9; N, 12.2. Found : C, 34.5; H, 3.7; N, 12.0. IR (ATR): 3093m, 2966w, 1628s, 1604m, 1543w, 1476s, 1445m, 1395w, 1381w, 1288s, 1234w, 1191w, 1154w, 1128s, 1034w, 1027w, 915w, 816w, 766m, 743w, 696w cm⁻¹.

[(LCu)₂Dy(NO₃)₃(H₂O)]. 10 Yield : (75 %). Anal. Calcd for C₃₀H₄₀Cu₂DyN₉O₁₄: (1040.3) C, 34.6; H, 3.9; N, 12.1. Found : C, 34.4; H, 3.6; N, 11.9. IR (ATR): 3100l, 2965w, 1628s, 1604m, 1543w, 1477s, 1445m, 1395w, 1381w, 1289s, 1224w, 1191w, 1154w, 1128s, 1034w, 1027w, 914w, 816w, 766m, 745w, 695w cm⁻¹.

[(LCu)₂Ho(NO₃)₃(H₂O)]. 11 Yield : (72 %). Anal. Calcd for C₃₀H₄₀Cu₂HoN₉O₁₄: (1042.7) C, 34.6; H, 3.9; N, 12.1. Found : C, 34.2; H, 3.5; N, 11.7. IR (ATR): 3100l, 2965w, 1628s, 1604m, 1543w, 1478s, 1445m, 1395w, 1381w, 1289s, 1224w, 1191w, 1154w, 1128s, 1034w, 1027w, 914w, 816w, 766m, 746w, 695w cm⁻¹.

[(LCu)₂Y(NO₃)₃(H₂O)](C₃H₆O). 12 Yield : (80 %). Anal. Calcd for C₃₃H₄₆Cu₂N₉O₁₅Y (1024.8) C, 38.7; H, 4.5; N, 12.3. Found : C, 38.2; H, 4.3; N, 12.0. IR (ATR): 3100l, 2972w, 1711m, 1629s, 1602m, 1543w, 1492m, 1469s, 1448s, 1397w, 1383w, 1295s, 1223w, 1188w, 1142m, 1127m, 1036m, 1004w, 915w, 817w, 757m, 747w, 696w cm⁻¹.

[LCuHo(NO₃)₃(H₂O)₂(C₃H₆O)]. 13 Recrystallization in open atmosphere of an acetone solution of [(LCu)₂Ho(NO₃)₃(H₂O)] yielded only a few crystals of **13** suitable for XRD and IR data. IR (ATR): 3422s, 2978w, 1683m, 1661w, 1629s, 1602m, 1459s, 1446s, 1334s, 1280s, 1216m, 1189w, 1127m, 1028m, 914w, 814w, 766m, 741w, 697w cm⁻¹.

[LCuEr(NO₃)₃(H₂O)₂(C₃H₆O)]. 14¹⁴ Yield : (76 %). Anal. Calcd for C₁₈H₂₉CuErN₆O₁₄ (784.3) C, 27.6; H, 3.7; N, 10.7. Found : C, 34.4; H, 3.5; N, 10.3. IR (ATR): 3421s, 2977w, 1682m, 1661w, 1629s, 1602m, 1547w, 1459s, 1446s, 1334s, 1281s, 1216m, 1189w, 1126m, 1028m, 914w, 814w, 766m, 741w, 697w cm⁻¹.

[LCuYb(NO₃)₃(H₂O)₂(C₃H₆O)]. 15¹⁴ Yield : (71 %). Anal. Calcd for C₁₈H₂₉CuN₆O₁₄Yb (790.0) C, 27.4; H, 3.7; N, 10.6. Found : C, 27.2; H, 3.6; N, 10.2. IR (ATR): 3410s, 2978w, 1683m, 1661w, 1630s, 1602m, 1548w, 1446s, 1335s, 1283s, 1215m, 1189w, 1127m, 1029m, 914w, 814w, 766m, 743w, 698w cm⁻¹.

Physical Measurements.

C, H, and N elemental analyses were carried out at the Laboratoire de Chimie de Coordination Microanalytical Laboratory in Toulouse, France. IR spectra were recorded with a Perkin-Elmer Spectrum 100FTIR using the ATR mode. The cell parameters for **8** were determined by powder X-ray diffraction at room temperature using a MPDPro Panalytical diffractometer equipped with a linear Xcelerator detector with CuK α (1.54056 Å). Indexing was realized by use of the DICVOL(1) program¹⁹ and the obtained unit cell parameters were refined with the X'pert Highscore program.²⁰ Magnetic data were obtained with a Quantum Design MPMS SQUID susceptometer. Magnetic susceptibility measurements were performed in the 2-300 K temperature range under a 0.1 T applied magnetic field, and diamagnetic corrections were applied by using Pascal's constants.²¹ Isothermal magnetization measurements were performed up to 5 T at 2 K. The magnetic susceptibilities have been computed by exact calculations of the energy levels associated to the spin Hamiltonian through diagonalization of the full matrix with a general program for axial symmetry,²² and with the MAGPACK program package²³ in the case of magnetization. Least-squares fittings were accomplished with an adapted version of the function-minimization program MINUIT.²⁴

Crystallographic Data Collection and Structure Determination for the complexes **1**, **9** and **13**.

Crystals of **1**, **9** and **13** were kept in the mother liquor until they were dipped into oil. The chosen crystals were mounted on a Mitegen micromount and quickly cooled down to 180 K (**1**, **9**) or 100 K (**13**). The selected crystals of **1** (pale red, 0.30 × 0.10 × 0.02 mm³), **9** (green, 0.20 × 0.12 × 0.04 mm³) and **13** (pink, 0.20 × 0.15 × 0.02 mm³) were mounted on an Oxford-

Diffraction Gemini (**1**) or a Bruker Kappa Apex II (**9**, **13**) using a graphite monochromator ($\lambda = 0.71073 \text{ \AA}$) and equipped with an Oxford Cryosystems cooler device. The unit cell determination and data integration were carried out using CrysAlis RED or SAINT packages.²⁵⁻²⁷ The structures have been solved using SUPERFLIP²⁸ or SHELXS-97²⁹ and refined by least-squares procedures using the software packages CRYSTALS³⁰ or WinGX version 1.63.³¹ Atomic Scattering Factors were taken from the International tables for X-Ray Crystallography.³² All hydrogen atoms were geometrically placed and refined by using a riding model. All non-hydrogen atoms were anisotropically refined. Drawings of molecules are performed with the program CAMERON³³ with 30% probability displacement ellipsoids for non-hydrogen atoms.

Crystal data for 1: $C_{30}H_{38}Cu_2N_6O_4$, $M = 673.76$, triclinic, P-1 (No.2), $Z = 1$, $a = 7.6254(8)$, $b = 9.6654(10)$, $c = 10.4451(12) \text{ \AA}$, $\alpha = 90.651(9)^\circ$, $\beta = 108.055(10)^\circ$, $\gamma = 100.708(9)^\circ$, $V = 717.21(14) \text{ \AA}^3$, 9078 collected reflections, 2619 unique reflections ($R_{\text{int}} = 0.1003$), R-factor = 0.052, weighted R-factor = 0.058 for 1608 contributing reflections [$I > 3\sigma(I)$].

Crystal data for 9: $C_{30}H_{40}Cu_2N_9O_{14}Tb$, $M = 1036.71$, monoclinic, $P2_1/c$ (No.14), $Z = 4$, $a = 11.9478(5)$, $b = 18.4048(7)$, $c = 17.5548(7) \text{ \AA}$, $\beta = 96.735(2)^\circ$, $V = 3833.6(3) \text{ \AA}^3$, 64206 collected reflections, 7830 unique reflections ($R_{\text{int}} = 0.0293$), $R = 0.0164$, $R_w = 0.0391$ for 7080 contributing reflections [$I > 2\sigma(I)$].

Crystal data for 13: $C_{18}H_{29}Cu_2HoN_6O_{14}$, $M = 781.94$, triclinic, P-1 (No.2), $Z = 2$, $a = 10.5144(4)$, $b = 11.4478(4)$, $c = 11.5167(4) \text{ \AA}$, $\alpha = 86.825(2)^\circ$, $\beta = 85.037(2)^\circ$, $\gamma = 89.709(2)^\circ$, $V = 1378.91(9) \text{ \AA}^3$, 35046 collected reflections, 12207 unique reflections ($R_{\text{int}} = 0.0310$), R-factor = 0.026, weighted R-factor = 0.023 for 9933 contributing reflections [$I > 3\sigma(I)$].

Results and Discussion

Syntheses

The preparation of the non symmetrical Schiff base complex LCu possessing a phenol and an oxime function was described earlier. In a previous work we showed that the LCu starting complex reacts with early and late Ln ions to yield trinuclear $[(LCu)_2Ce(NO_3)_3]^{12}$ and dinuclear $[(LCuEr(NO_3)_3(H_2O)_2)]$ or $[(LCuYb(NO_3)_3(H_2O)_2)]^{14}$ complexes. At that time, we only knew that use of $Gd(NO_3)_3 \cdot 5H_2O$ yielded trinuclear complexes but we could not isolate crystals suitable for XRD. Fortunately, use of $Tb(NO_3)_3 \cdot 5H_2O$ was more successful and allowed us to confirm the trinuclear structure of the isolated complex while powder X-Ray data showed that the corresponding Gd **8** and the Tb **9** complexes are isostructural. Infrared

data (Supplementary Material, Figure S1) allow to confirm that the series can be subdivided in three subseries. The first one goes from La to Eu, with complexes formulated $[(\text{LCu})_2\text{Ln}(\text{NO}_3)_3]$ devoid of water molecules. The second one spreads from Gd to Ho and involves the Y complex. These complexes are again trinuclear and correspond to $[(\text{LCu})_2\text{Ln}(\text{NO}_3)_3(\text{H}_2\text{O})]$ formulae, with a water molecule present in each case. Starting with Ho, the late Ln complexes become dinuclear, with $[(\text{LCuLn}(\text{NO}_3)_3(\text{H}_2\text{O})_2(\text{C}_3\text{H}_6\text{O}))]$ formulations and two water molecules bound to the Ln ions.

Structural characterizations

The crystallographic data of complexes **1**, **9** and **13** appear in the experimental section while views of the structures are reported in Figures 1, 2 and 3 respectively. Relevant bond distances and angles are collated in the corresponding figure captions. The structure of the starting copper complex **1** does confirm the non symmetrical character of the Schiff base ligand, with the copper ion linked to the phenoxo oxygen atom, to two imine nitrogen atoms and to the nitrogen atom of the oxime function. Two LCu units are positioned in a head to tail arrangement so that the phenoxo oxygen atom linked to a copper ion in the basal plane is also linked in axial position to the second Cu ion, thus yielding five-coordinate copper ions, with an axial Cu-O bond length (2.572(4) Å) larger than the equatorial one (1.910(4) Å). The

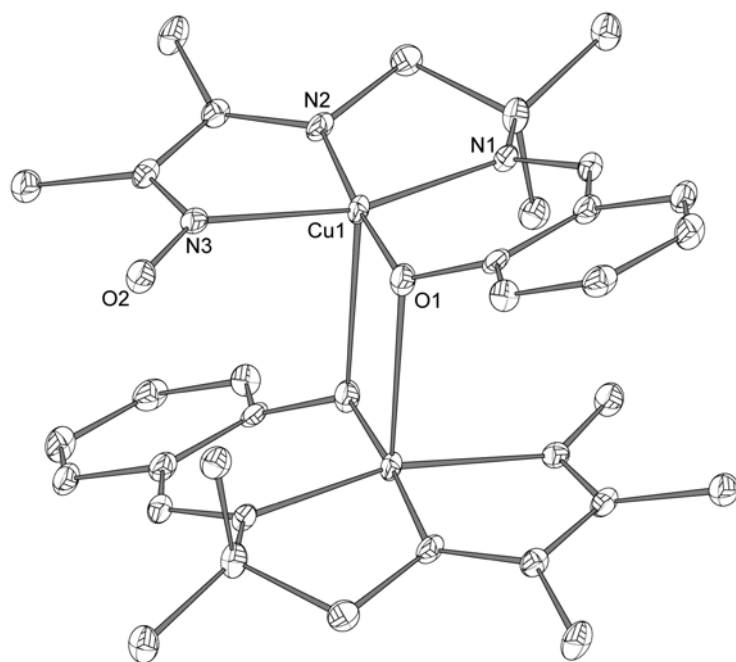


Figure 1. View of the dinuclear $[\text{LCu}]_2$ complex **1**. Selected bond lengths (Å) and angles (°): Cu N1 1.968(4), Cu N2 1.929(4), Cu N3 2.034(4), Cu O1 1.910(4), Cu O1' 2.572(4), N3 O2 1.267(6), Cu1...Cu1' 3.227(1) Å, O1 Cu N3 100.9(2), O1 Cu1 O1' 89.1(1), Cu O1 Cu' 90.9(1), Cu N3 O2 126.9(3)°.

resulting centrosymmetric dinuclear [LCu]₂ entity is made of LCu units that only differ by their non planar five-membered ring formed by the diamine moiety chelating the copper ion, with a δ gauche conformation in one unit and a λ gauche conformation in the other one. The axial bond is weak for the copper ions deviate only by 0.1044(7) Å from the mean N₃O coordination plane, but the presence of 5, 5, 6-membered cycles around the Cu ion induces a folding of the ligand. Surprisingly the deprotonated oxygen atom of the oxime function is not involved in hydrogen bonds, and there are only weak CH...O contacts that assemble these dinuclear entities into a 1-D chain. In the molecule the Cu...Cu distance is equal to 3.227(1) Å while the Cu...Cu distance between two molecules is larger, 4.998(2) Å.

Complex **9** is made of two LCu units linked to a Tb ion by the oxygen atom of their oxime function (Figure 2). Three nitrate anions chelate the Tb ion, which is also coordinated to a

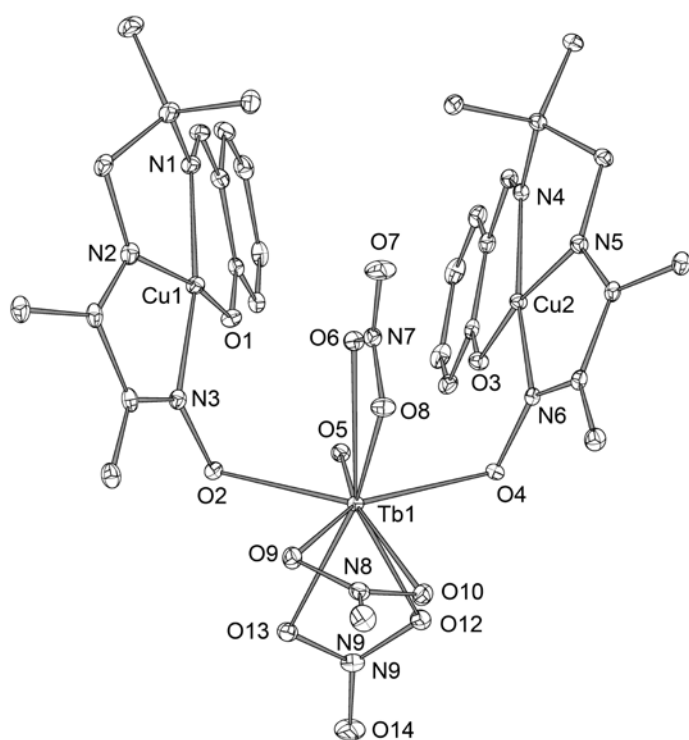


Figure 2. View of the trinuclear [Cu-Tb-Cu] complex **9**. Selected bond lengths (Å) and angles (°): Cu1 N1 1.949(2), Cu1 N2 1.948(2), Cu1 N3 1.996(2), Cu1 O1 1.893(1), N3 O2 1.330(2), Cu2 N4 1.939(2), Cu2 N5 1.934(2), Cu2 N6 1.983(2), Cu2 O3 1.981(2), N6 O4 1.334(2), Tb O2 2.295(1), Tb O4 2.272(1), Tb O5 2.380(1), Tb O6 2.577(1), Tb O8 2.489(1), Tb O9 2.471(1), Tb O10 2.507(1), Tb O12 2.486(1), Tb O13 2.440(1) Å, O2 N3 Cu1 125.7(1), O4 N6 Cu2 124.5(1), N3O2 Tb 126.5(1), N6 O4 Tb 127.9(1)°.

water molecule, thus yielding a nine-coordinate Tb ion. The water molecule is involved in two hydrogen bonds with each phenoxo oxygen atom of the two LCu units ($O1...O5 = 2.720(2)$, $O3...O5 = 2.714(2)$ Å), so that the Tb and Cu ions are doubly-bridged through the Cu-N-O-Tb oxime function and through the $Cu1(2)-O1(3)...H-O_w5-Tb$ hydrogen bond ($Gd-O5 = 2.380(1)$ Å). There is no direct link between the two copper ions, separated by a Cu...Cu distance of $5.1840(4)$ Å. One copper ion (Cu2) is four-coordinate, with a square planar environment while the other one (Cu1) presents a weak axial coordination with the oxygen atom O6 of a chelating nitrate anion, the Cu...O6 distance being large, $2.702(1)$ Å. Complexation of the Tb ion to the LCu units induces a slight shortening of the Cu-N and Cu-O bonds and an increase of the N-O oxime bond, from $1.267(6)$ to $1.330(2)$ or $1.334(2)$ Å. As usual, the Tb-O bond lengths depend on the nature of the oxygen atoms. The shortest bonds are the oximate Tb-O2(4) bonds ($2.295(1)$ and $2.272(1)$ Å) while the Tb-O5 water bond length is equal to $2.380(1)$ Å. The lengths of the Tb-O (nitrate) bonds vary from $2.440(1)$ Å to $2.508(1)$ Å, the bond involving the oxygen atom O6 in weak contact with the copper ion Cu1 being slightly larger, $2.577(1)$ Å. The bridging network Cu-N-O-Tb is not planar but the Cu-N-O and N-O-Tb angles are quite identical, $124.5(1)$, $125.7(1)^\circ$ and $126.5(1)$ and $127.9(1)^\circ$, respectively. The intramolecular Cu1(2)...Tb separations vary from $4.304(1)$ Å to $4.348(1)$ Å. CH...O contacts with the oxygen atoms of the nitrate anions create 1D chains, with intrachain metal...metal separations of $11.6156(3)$ Å and also short interchain Cu...Cu contacts ($4.079(4)$ Å, the corresponding Tb...Tb contacts being of $8.8176(4)$ Å).

Although we could not isolate crystals suitable for XRD, powder X-Ray data of the corresponding trinuclear $[(LCu)_2Gd(NO_3)_3(H_2O)]$ complex **8** confirm that this complex is isostructural with the trinuclear $[(LCu)_2Tb(NO_3)_3(H_2O)]$ complex **9** described above (Figure S2). Indeed the obtained unit cell parameters for **8** are in complete agreement with those of complex **9** (Table S1).

Complex **13** has several common features with the complex described above. The molecular structure corresponds to the $LCu1Tb(NO_3)_3(H_2O)$ part of complex **9** along with a supplementary water molecule that replaces the square planar LCu2 unit of **9**, as shown in Figure 3. The Cu and the Ho coordination spheres and the Cu-N, Cu-O and Ho-O bond lengths are quite comparable. The main difference concerns the hydrogen bonding. Two $[LCuHo(NO_3)_3(H_2O)_2]$ units are hydrogen bonded by their second water molecule through two acetone molecules, thus yielding a double $Ho-(H_2O)...O(acetone)...(H_2O)-Ho$ hydrogen bond with a Ho...Ho distance of $7.177(1)$ Å. As the first water molecule is still hydrogen bonded to the phenoxo oxygen atom and to a non coordinated oxygen atom of a nitrate anion

belonging to the next LCu unit, the resulting tetranuclear units are linked together to give 1D chains, with intrachain Ho...Ho and Cu...Cu distances of 8.291(1) and 10.514(1) Å. The shortest interchain Cu...Cu distance is equal to 7.923(1) Å.

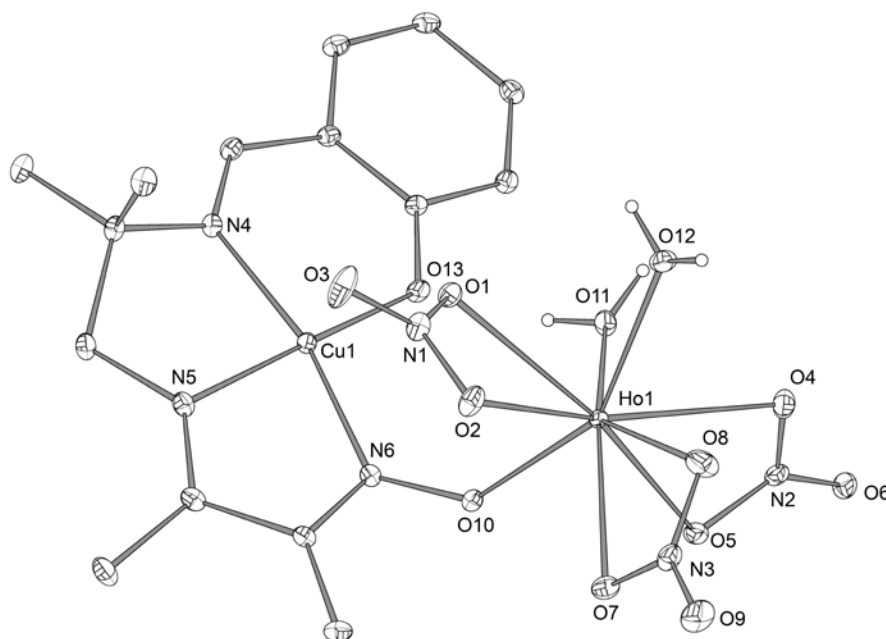
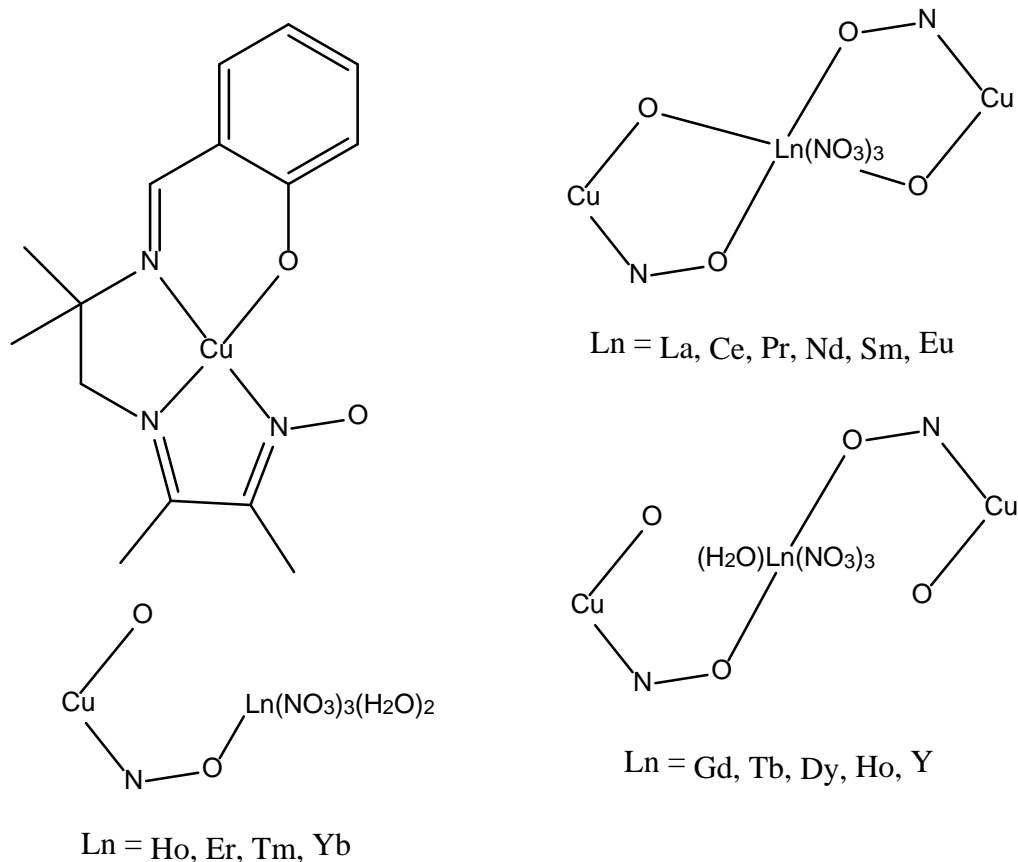


Figure 3. View of the dinuclear $[\text{LCuHo}(\text{NO}_3)_3(\text{H}_2\text{O})_2(\text{C}_3\text{H}_6\text{O})]$ complex **13**. Selected bond lengths (Å) and angles ($^\circ$): Cu N4 1.955(2), Cu N5 1.935(2), Cu N6 2.002(2), Cu O13 1.892(2), Cu O1 2.785(2), N6 O10 1.335(2), Ho O1 2.461(1), Ho O2 2.422(1), Ho O4 2.471(2), Ho O5 2.466(1), Ho O7 2.452(1), Ho O8 2.462(2), Ho O10 2.216(1), Ho O11 2.311(1), Ho O12 2.353(1), Cu...Ho 4.272(1) Å, O13 Cu N6 101.1(1), Cu N6 O10 127.3(1), N6 O10 Ho 127.3(1) $^\circ$.

In conclusion of the structural study, we have seen that complex **1** corresponds to the assembling of two asymmetric units that are δ and λ gauche conformers. We can notice the non participation of the phenoxo oxygen atom to the complexation of the Tb ion in complex **9** and the presence of two bridges between the Tb and each Cu ions, the oxime Cu-N-O-Ln bridge and a Tb-O_w-H...O-Cu bridge involving a hydrogen bond, each bridge being characterized by similar geometrical parameters, bond lengths and angles. A similar copper-holmium bridging is present in complex **13**. Although we could not obtain crystals suitable for a structural determination of the corresponding copper-gadolinium complex **8**, powder X-Ray diffraction measurements did confirm that the complexes $[(\text{LCu})_2\text{Tb}(\text{NO}_3)_3(\text{H}_2\text{O})]$ and $[(\text{LCu})_2\text{Gd}(\text{NO}_3)_3(\text{H}_2\text{O})]$ are isostructural, and these structural analogies are useful to interpret the magnetic behavior. The copper complex used as ligand and its coordination to Ln ions all along the Ln series are summarized in Scheme 1.



Scheme 1. Schematic representation of the Cu complex used as ligand and its coordination to Ln ions all along the Ln series.

Magnetic properties.

We report in Figures 4-8 the magnetic behaviors of complexes **1**, **2**, **8**, **12** in the form of the thermal variation of the $\chi_M T$ product (χ_M is the molar magnetic susceptibility corrected for the diamagnetism of the ligands).²¹ In complex **1** the $\chi_M T$ product, which is equal to $0.79 \text{ cm}^3 \text{ mol}^{-1} \text{ K}$ at 300 K stays practically constant till to 50 K ($0.75 \text{ cm}^3 \text{ mol}^{-1} \text{ K}$), decreases smoothly between 50 and 20 K ($0.67 \text{ cm}^3 \text{ mol}^{-1} \text{ K}$), and more abruptly till 2 K where it is equal

to $0.12 \text{ cm}^3\text{mol}^{-1}\text{K}$ (Figure 4). The $\chi_M T$ at room temperature is in the range of the

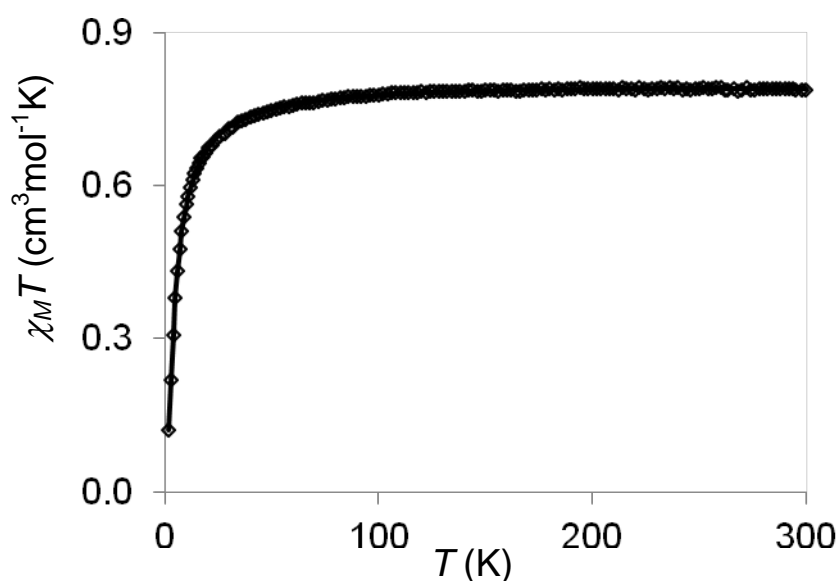


Figure 4. Temperature dependence of the $\chi_M T$ product for complex **1** at 0.1 T applied magnetic field. The solid line corresponds to the best data fit (see text).

expected value for two isolated Cu ions ($0.75 \text{ cm}^3\text{mol}^{-1}\text{K}$ with $g = 2$). In view of the structure described above, a qualitative analysis was performed with a simple isotropic Hamiltonian $H = -2J(S_{\text{Cu}1} \cdot S_{\text{Cu}2})$. The resulting interaction parameter is very weak, $J_{\text{CuCu}} = -2.62 \text{ cm}^{-1}$, with $g = 2.05$ and a nice agreement factor $R = \sum [(\chi_M T)_{\text{obs}} - (\chi_M T)_{\text{calc}}]^2 / \sum [(\chi_M T)_{\text{obs}}]^2$ equal to 1×10^{-5} . Complexes **2** and **12** correspond also to dinuclear Cu complexes, in which the two Cu ions are separated by a diamagnetic La or Y ion. In complex **2** the $\chi_M T$ product behaves as in complex **1**, being equal to $0.84 \text{ cm}^3\text{mol}^{-1}\text{K}$ at 300 K, $0.75 \text{ cm}^3\text{mol}^{-1}\text{K}$ to 50 K and $0.36 \text{ cm}^3\text{mol}^{-1}\text{K}$ at 2 K (Figure 5). Using the same Hamiltonian yields $J_{\text{CuCu}} = -1.28 \text{ cm}^{-1}$, with $g = 2.05$, TIP (temperature independent paramagnetism) = $0.2 \cdot 10^{-3}$ and $R = 2.2 \cdot 10^{-4}$. For complex **12** (Figure 6), the $\chi_M T$ product remains constant from 300 to 8 K ($0.76 \text{ cm}^3\text{mol}^{-1}\text{K}$) and slightly decreases to $0.72 \text{ cm}^3\text{mol}^{-1}\text{K}$ at 2 K, thus confirming absence of interaction in that complex. These two results are quite informative. In view of the structural determinations, we know that the La ion bridges two Cu ions through the phenoxo and oximato bridges in **2** and that the Y ion bridges the two Cu ions through the oximato bridge and the hydrogen bond, complexes **12** and **9** being isostructural. This means that a weak Cu-Cu antiferromagnetic

interaction is transmitted by the phenoxo bridge and the diamagnetic La ion in the

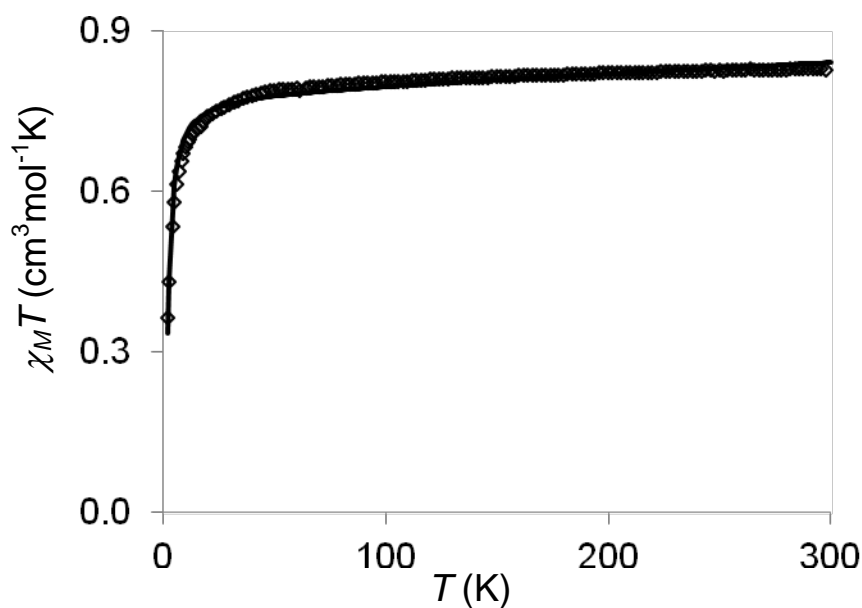


Figure 5. Temperature dependence of the $\chi_M T$ product for complex **2** at 0.1 T applied magnetic field. The solid line corresponds to the best data fit (see text).

[(LCu)₂La(NO₃)₃] complex **2**, the oximato bridge being unable to transmit interaction through the diamagnetic Y ion in complex **12**. The result will be useful for the understanding of the magnetic behavior in complex **8**.

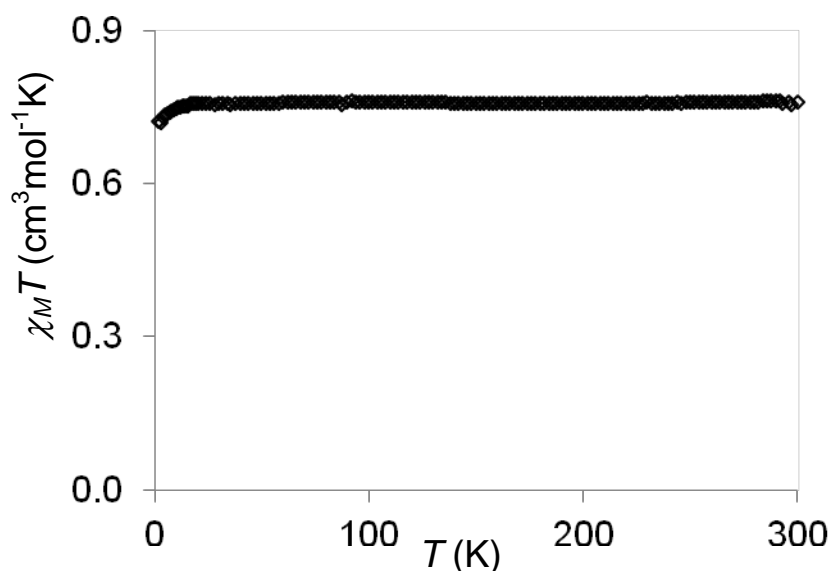


Figure 6. Temperature dependence of the $\chi_M T$ product for complex **12** at 0.1 T applied magnetic field.

For complex **8**, the $\chi_M T$ product, which is equal to $8.54 \text{ cm}^3 \text{mol}^{-1} \text{K}$ at 300 K, is not far from the value expected for non interacting Cu and Gd ions ($8.62 \text{ cm}^3 \text{mol}^{-1} \text{K}$). It remains

constant till 100 K ($8.41 \text{ cm}^3 \text{ mol}^{-1} \text{ K}$), then slowly decreases till 30 K ($8.00 \text{ cm}^3 \text{ mol}^{-1} \text{ K}$) before starting a sharp decrease to $4.57 \text{ cm}^3 \text{ mol}^{-1} \text{ K}$ at 2 K (Figure 7). The structural determination

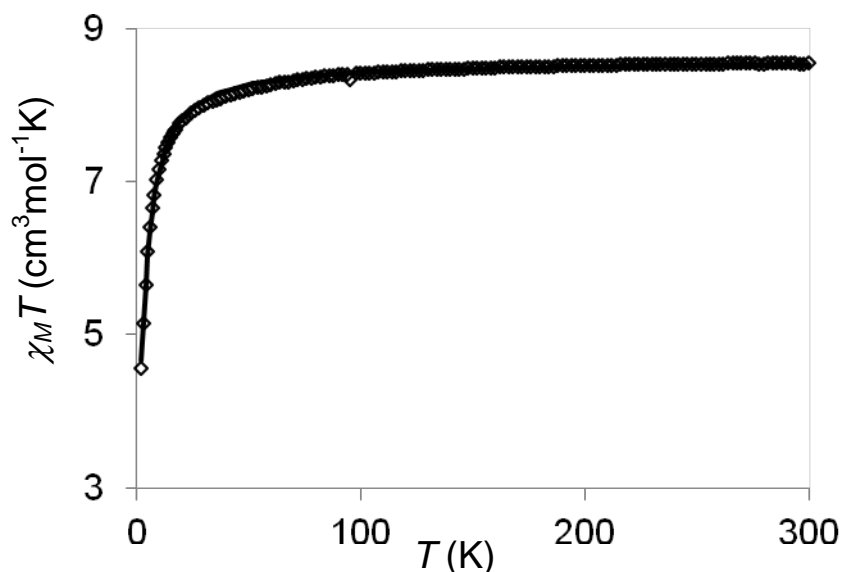


Figure 7. Temperature dependence of the $\chi_M T$ product for complex **8** at 0.1 T applied magnetic field. The solid line corresponds to the best data fit: $J_{\text{Cu-Gd}} = -0.63 \text{ cm}^{-1}$, $g = 2.00$.

shows that two interaction pathways can be active, through the oximate bridge and through the hydrogen bond. The calculated J parameter corresponds to the overall Cu-Gd interaction present in complex **8**, the oximate bridge playing of course the main role. In view of the magnetic behavior of complex **12**, we know that we have not to consider a Cu-Cu interaction. So the analysis is realized with the following Hamiltonian including Zeeman and isotropic exchange terms $H = -2J(S_{\text{Cu1}} \cdot S_{\text{Gd}} + S_{\text{Cu2}} \cdot S_{\text{Gd}})$, with intermolecular interactions taken into account as usual. The parameter values corresponding to the best fit are: $J_{\text{Cu-Gd}} = -0.63 \text{ cm}^{-1}$, $g = 2.00$, $R = 2 \times 10^{-5}$, and negligible paramagnetic contribution (PAR), temperature independent parameter (TIP) and intermolecular interactions. So it becomes evident that the Cu-Gd interaction through the oximate bridge is antiferromagnetic.

The temperature dependence of the the $\chi_M T$ product for complexes **9** is given in the Supplementary Material, Figure S3. The 300 K value ($12.40 \text{ cm}^3 \text{ mol}^{-1} \text{ K}$) corresponds to what is expected for two Cu and one Tb non interacting ions ($12.57 \text{ cm}^3 \text{ mol}^{-1} \text{ K}$). At 100 K a value of $11.9 \text{ cm}^3 \text{ mol}^{-1} \text{ K}$ is observed before a regular decrease till 20 K ($9.7 \text{ cm}^3 \text{ mol}^{-1} \text{ K}$) followed by a sharp decrease to $5.56 \text{ cm}^3 \text{ mol}^{-1} \text{ K}$ at 2 K. A similar behavior is observed for complex $[(\text{LCu})_2\text{Dy}(\text{NO}_3)_3(\text{H}_2\text{O})]$ **10** but interpretation of these data is not easy, the Tb and Dy ions possessing first-order angular moments precluding use of spin-only Hamiltonians. The strong

anisotropy induces a decrease of the $\chi_M T$ product at low temperature and absence of saturation in the magnetization curves for these complexes **9** and **10**. So, in view of the magnetic behavior of complex **8**, nothing can be told about the Cu-Tb or Cu-Dy magnetic interaction. Nevertheless we had a look at the dynamic magnetic properties of these two complexes. The ac susceptibility measurements for **9** and **10** show frequency-dependent signals, suggesting SMM behavior, but we could not observe maxima for the out-of-phase signals above 2 K, even after application of a 0.1 T field (see Figure S4, Supplementary Material). Due to the poor SMM behavior of these complexes, their study has not been completed.

Discussion

The oxime function has been largely used by V. Pecoraro to obtain a huge number of metallo-crown complexes and particularly to prepare heteronuclear 3d-4f complexes in which the 4f ion is surrounded and bridged to a variable number of 3d ions through oxime bridges, 5 in the complexes we are interested in.³⁴⁻³⁶ On the contrary, CuLn₄ complexes with a central Cu ion surrounded by four oxime functions bridging four Ln ions have also been obtained and studied for their magnetic properties.¹⁰ Till now there are only two examples of dinuclear complexes having a unique oxime bridge in between a 3d and a 4f ion. They concern the previously published Cu-Er and Cu-Yb complexes of this series.¹⁴ In the past, we have obtained non symmetrical ligands able to link Cu and Gd ions through a mixed double bridge involving a phenoxo oxygen atom on the one hand and an oxime function on the other hand.^{11,12} The magnetic behavior of the resulting complexes was puzzling for ferromagnetic and antiferromagnetic interactions were detected, depending on the used ligands.

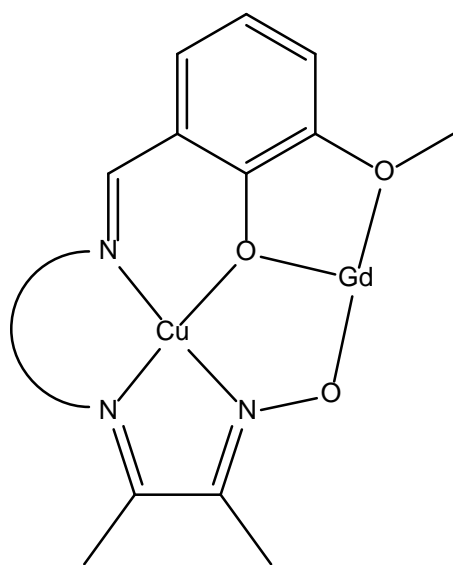
The aim of the present work is directed toward a better understanding of the magnetic interaction through the oxime bridge in Cu-Gd complexes. Indeed the metallo-crown Cu₅-Gd entities,³⁴ as the Cu-Gd₄ complex¹⁰ indicate that weak antiferromagnetic interactions are active, contrary to what is observed in a large majority of Cu-Gd complexes. The presence of Gd-Gd interactions along with the Cu-Gd interactions in the Cu-Gd₄ compounds can be retained to explain this change, although such an explanation does not hold for the metallo-crown species. We tried to simplify the problem in preparing complexes with a low number of metal ions, the best example being given by well isolated heterodinuclear Cu-Gd complexes. This is why we studied the reaction of the ligand complex **1**, [LCu]₂ with the series of Ln ions. Unfortunately, we have not succeeded in the preparation of such complexes for, in the Gd case, a trinuclear Cu-Gd-Cu compound **8** is characterized.

The structural determinations of the isolated complexes do confirm that the main difference between the trinuclear complexes implying early Ln ions till Europium and those obtained with Gd, Tb, Dy, Ho and Y ions is the disappearance of the two Cu-phenoxo-Ln bridge, which are replaced by two Ln-OH₂ ...O(phenoxo)-Cu hydrogen bonds. On the contrary, dinuclear complexes are isolated on going from Ho to late Ln ions, the LCu square planar entity coordinated to the Ln ion being replaced by a water molecule that is hydrogen-bonded to an acetone molecule. So we observe three types of structures all along the Ln series: trinuclear Cu-Ln-Cu type 1 complexes with a double phenoxo-oximato Cu-Ln bridge with Ln = La, Ce, Pr, Nd, Sm, Eu; trinuclear Cu-Ln-Cu type 2 complexes with a unique oximato Cu-Ln bridge, the Cu-phenoxo-Ln bridge being replaced by a Ln-OH₂ ...O(phenoxo)-Cu hydrogen bond with Ln = Gd, Tb, Dy, Ho, Y; dinuclear Cu-Ln type 3 complexes with a unique oximato Cu-Ln bridge with Ln = Ho, Er, Tm, Yb (see Scheme 1). In these last complexes, the water molecule, which was hydrogen-bonded to the phenoxo oxygen atoms of each LCu units, is now hydrogen-bonded to the remaining LCu unit and to a non coordinated oxygen atom of a nitrate anion, the other water molecule being hydrogen-bonded to an acetone molecule. We also must remember that crystallization of trinuclear complexes **8**, **9** is very difficult, contrary to crystallization of the dinuclear species involving the late Ln ions. This is why recrystallization of the Ho complex, which is located at the limit of type 2 and type 3 complexes, gave only a few crystals of [(LCu)Ho(NO₃)₂(H₂O)₂(C₃H₆O)] while the main product does correspond to the trinuclear [(LCu)₂Ho(NO₃)₃(H₂O)] entity. Fortunately the dinuclear species are easily recognized with help of their infrared spectra, the water molecules giving a nice peak at 3420-3410 cm⁻¹ and the keto function of the hydrogen-bonded acetone appearing at 1682 cm⁻¹ instead of 1711 cm⁻¹ for solvated acetone.

The magnetic studies indicate that a weak antiferromagnetic Cu-Cu interaction is active in [(LCu)₂La(NO₃)₃] complex **2**, where the copper ions are linked through the diamagnetic La ion by a double phenoxo-oximato bridge. On the contrary, the two copper ions are well isolated in the trinuclear [(LCu)₂Y(NO₃)₃(H₂O)](C₃H₆O) complex **12** in which the Cu-O(phenoxo)-Y bridge is replaced by a Cu-O(phenoxo)...(H₂O)-Y hydrogen-bond. Thanks to the magnetic behavior of this trinuclear Cu-Y-Cu compound, we know that the Cu...Cu interaction can be eliminated, and that the weak antiferromagnetic Cu-Cu interaction observed in the trinuclear [(LCu)₂La(NO₃)₃] complex is supported by the Cu-O-La-O-Cu double phenoxo bridge. If we come back to the trinuclear [(LCu)₂Gd(NO₃)₃(H₂O)] complex **8**, the observed antiferromagnetic interaction must be associated to the Cu-N-O-Gd oximato bridge, the only one to be active in compound **8**. We must also recall that this result is in complete

agreement with the magnetic study of the Cu-Gd₄ complex, in which the Cu and Gd ions are bridged with a double oximato bridge.¹⁰ Furthermore, the antiferromagnetic Cu-Gd interaction present in the CuGd₄ complex was also confirmed by an EPR study.³⁷

This result allows us to reinvestigate the magnetic behavior of complexes we published previously. Indeed, in the past, we prepared non symmetric ligands yielding Cu-Gd complexes in which the Cu and Gd ions are bridged by a phenoxo and an oximato bridge.^{11,12} We could characterize two families of dinuclear Cu-Gd and trinuclear Cu-Gd-Cu complexes. At that time, we explained the different magnetic behavior, from ferromagnetic to antiferromagnetic, by the variation of the hinge angle, the dihedral angle between the O-Cu-N



Scheme 2. Schematized complexes with diamino chains (half-circle) involving 2 or 3 carbon atoms.

and O-Gd-O planes in the bridging core. Depending on the number of carbon atoms (2 or 3) in the diamino chain (see the half-circle in Scheme 2 that corresponds to -CH₂-C(Me)₂- or to -CH₂-C(Me)₂-CH₂-), the hinge angle varies from 6.1(1)° with two carbon atoms to 39.1(1)° with three carbon atoms involved in this chain. We also remarked previously that the strength of the interaction was correlated to the value of the hinge angle.⁵ This was more recently supported by DFT calculations, the magnetic interaction increasing with the planarity of the bridging fragment.^{7,15} With diphenoxo bridges, we always observed ferromagnetic Cu-Gd interactions varying from 10.1 cm⁻¹ for a hinge angle equal to 1.7(2)°⁵ to 0.20(4) cm⁻¹ for a hinge angle of 41.6(2)°.³⁸ We can now better understand why complexes involving a phenoxo and an oximato bridges show an overall ferro or antiferromagnetic interaction. In view of the results presented above, we know that such bridges have opposite effects on the magnetic

interaction. Indeed a hinge angle of 6.1° does favor a correct ferromagnetic interaction through the Cu-O(phenoxo)-Gd bridge that is able to overcome the antiferromagnetic interaction coming from the oximato bridge, thus explaining the net overall ferromagnetic interaction equal to $3.5(1) \text{ cm}^{-1}$.¹¹ On the contrary, a hinge angle of 39.1° largely decreases the contribution of the phenoxo bridge and the global Cu-Gd interaction becomes antiferromagnetic, $J = -0.49(1) \text{ cm}^{-1}$, as observed in the previously published complex.¹¹

Conclusion

Reaction of the LCu complex ligand with Ln ions allows characterization of three different structures all along the Ln series: trinuclear Cu-Ln-Cu type 1 complexes with a double phenoxo-oximato Cu-Ln bridge with Ln = La, Ce, Pr, Nd, Sm, Eu; trinuclear Cu-Ln-Cu type 2 complexes with a unique oximato Cu-Ln bridge, the Cu-phenoxo-Ln bridge being replaced by a Ln-OH₂ ...O(phenoxo)-Cu hydrogen bond; dinuclear Cu-Ln type 3 complexes with a unique oximato Cu-Ln bridge and a Ln-OH₂ ...O(phenoxo)-Cu hydrogen bond, the water molecules being hydrogen-bonded to an acetone molecule and to a non coordinated oxygen atom of a nitrate anion. Absence of a Cu-Cu magnetic interaction in the trinuclear Cu-Y-Cu complex does confirm that neither the double oximato Cu-N-O-Y-O-N-Cu bridges nor the double Ln-OH₂...O(phenoxo)-Cu hydrogen bonds are able to transmit a Cu-Cu magnetic interaction through the Y ion. As a consequence the antiferromagnetic interaction present in the trinuclear Cu-Gd-Cu complex can only be attributed to the oximato Cu-N-O-Gd bridge, in contrast to the ferromagnetic Cu-Gd interaction induced by the single oxygen atom phenoxo bridge in a lot of Cu-Gd complexes. This result allows to understand why complexes in which the Cu and Gd ions are simultaneously linked by a phenoxo and an oximato bridges can present ferro or antiferromagnetic Cu-Gd interactions. This experimental confirmation of an antiferromagnetic interaction through the two-atoms (nitrogen and oxygen) oximato bridge has to be taken into account in the building of novel 3d-Gd complexes.

Supporting Information. Electronic Supplementary Information (ESI) available: Supplementary Figures S1-S4.CCDC 996961 (Compound **1**), 996962 (Compound **9**), 996963 (Compound **13**). For ESI and crystallographic data in CIF format see ...

Acknowledgments

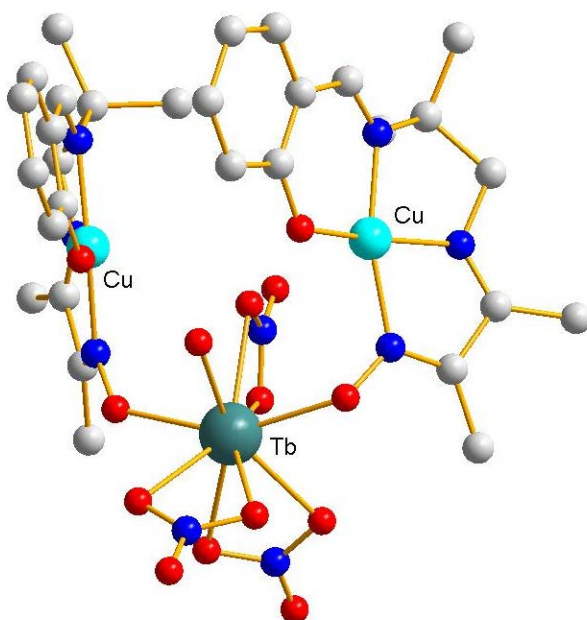
This work was supported by CNRS and MAGMANet (Grant NMP3-CT-2005-515767), The authors are grateful to Dr. A. Mari for technical assistance.

References

- 1 C. Benelli, D. Gatteschi, *Chem. Rev.* **2002**, *102*, 2369.
- 2 M. Andruh, J. P. Costes, C. Diaz, S. Gao, *Inorg. Chem.* **2009**, *42*, 268.
- 3 R. Sessoli, A. K. Powell, *Coord. Chem. Rev.* **2009**, *253*, 2328.
- 4 Y. G. Huang, F. L. Jiang, M. C. Hong, *Coord. Chem. Rev.* **2009**, *253*, 2814.
- 5 J. P. Costes, F. Dahan, A. Dupuis, A. *Inorg. Chem.* **2000**, *39*, 165-168.
- 6 J. P. Costes, F. Dahan, A. Dupuis, A., J. P. Laurent, *Inorg. Chem.* **1997**, *36*, 4284-4286.
- 7 E. Colacio, J. Ruiz, A. J. Mota, M. A. Palacios, E. Cremades, E. Ruiz, F. J. White, E. K. Brechin, *Inorg. Chem.* **2012**, *51*, 5857-5868.
- 8 a) V. Gomez, L. Vendier, M. Corbella, J. P. Costes, *Inorg. Chem.* **2012**, *51*, 6396-6404 ; b) E. Colacio, J. Ruiz, A. J. Mota, M. A. Palacios, E. Ruiz, E. Cremades, M. M. Hänninen, R. Sillanpää, E. K. Brechin, *Comptes Rendus Chimie*, 2012, *15*, 878-888.
- 9 A. Okazawa, T. Nogami, H. Nojiri, T. Ishida, *Chem. Mater.* **2008**, *20*, 3110-3119.
- 10 Y. Kobayashi, S. Ueki, T. Ishida, T. Nogami, *Chem. Phys. Lett.* **2003**, *378*, 337-342.
- 11 J. P. Costes, F. Dahan, A. Dupuis, A., J. P. Laurent, *Inorg. Chem.* **2000**, *39*, 169-173.
- 12 J. P. Costes, F. Dahan, A. Dupuis, A., *Inorg. Chem.* **2000**, *39*, 5994-6000.
- 13 S. Ueki, Y. Kobayashi, T. Ishida, T. Nogami, *Chem. Commun.* **2005**, 5223-5225.
- 14 J. P. Costes, L. Vendier, *C. R. Chimie*, **2010**, *13*, 661-667.
- 15 E. Cremades, S. Gomez-Coca, D. Aravena, S. Alvarez, E. Ruiz, *J. Am. Chem. Soc.* **2012**, *134*, 10532-10542.
- 16 M. F. Richardson, W. F. Wagner, D. E. Sands, *J. Inorg. Nucl. Chem.* **1968**, *30*, 1275-1280.
- 17 S. Sakamoto, T. Fujinami, K. Nishi, N. Matsumoto, N. Mochida, T. Ishida, Y. Sunatsuki, N. Re, *Inorg. Chem.* **2013**, *52*, 7218-7229.
- 18 J. A. Bevan, D. P. Graddon, J. F. McConnell, *Nature*, **1963**, *199*, 373.
- 19 A. Boultif, D. Louer, *J. Appl. Cryst.* **2004**, *37*, 724-731.
- 20 X'pert Highscore, Panalytical, 2008.
- 21 P. Pascal, *Ann. Chim. Phys.*, **1910**, *19*, 5-70.
- 22 A. K. Boudalis, J. M. Clemente-Juan, F. Dahan, J. P. Tuchagues, *Inorg. Chem.* **2004**, *43*, 1574-1586.
- 23 (a) J. J. Borrás-Almenar, J. M. Clemente-Juan, E. Coronado, B. S. Tsukerblat, *Inorg. Chem.* **1999**, *38*, 6081-6088. (b) J. J. Borrás-Almenar, J. M. Clemente-Juan, E. Coronado, B. S. Tsukerblat, *J. Comput. Chem.* **2001**, *22*, 985-991.

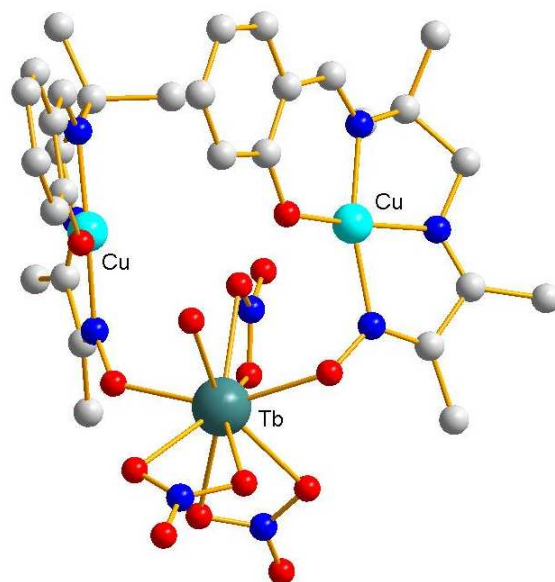
- 24 F. James, M. Roos, "MINUIT Program, a System for Function Minimization and Analysis of the Parameters Errors and Correlations"; *Comput. Phys. Commun.*, **1975**, *10*, 343-367.
- 25 Agilent Technologies (2011). Agilent Technologies UK Ltd., Oxford, UK, Xcalibur CCD system, CrysAlisPro Software system, Version 1.171.35.19.
- 26 **CrysAlis CCD, CrysAlis RED and associated programs:** Oxford Diffraction (2006). *Program name(s)*. Oxford Diffraction Ltd, Abingdon, England.
- 27 **SAINT** Bruker (2007). Bruker AXS Inc., Madison, Wisconsin, USA.
- 28 **Superflip** L. Palatinus, G. Chapuis, *J. Appl. Cryst.* **2007**, *40*, 786-790.
- 29 SHELX97 [Includes SHELXS97, SHELXL97, CIFTAB] - Programs for Crystal Structure Analysis (Release 97-2). G. M. Sheldrick, Institut für Anorganische Chemie der Universität, Tammanstrasse 4, D-3400 Göttingen, Germany, 1998.
- 30 **CRYSTALS:** P. W. Betteridge, J. R. Carruthers, R. I. Cooper, K. Prout, D. J. Watkin, *J. Appl. Cryst.* **2003**, *36*, 1487.
- 31 WINGX - 1.63 Integrated System of Windows Programs for the Solution, Refinement and Analysis of Single Crystal X-Ray Diffraction Data. L. Farrugia, *J. Appl. Crystallogr.* **1999**, *32*, 837-840.
- 32 International tables for X-Ray crystallography, Vol IV, Kynoch press, Birmingham, England, 1974.
- 33 **CAMERON** D. J. Watkin, C. K. Prout, L. J. Pearce, (1996). Chemical Crystallography Laboratory, Oxford, England.
- 34 C. M. Zaleski, C. S. Lim, A. D. Cutland-Van Noord, J. W. Kampf, V. L. Pecoraro, *Inorg. Chem.* **2011**, *50*, 7707-7717.
- 35 C. S. Lim, J. Jankolovits, J. W. Kampf, V. L. Pecoraro, *Inorg. Chem.* **2011**, *50*, 4832-4841.
- 36 A. J. Stemmler, J. W. Kampf, M. L. Kirk, B. L. Atasi, V. L. Pecoraro, *Inorg. Chem.* **1999**, *38*, 2807-2817.
- 37 K. Fujiwara, A. Okazawa, N. Kojima, G. Tanaka, S. Yoshii, H. Nojiri, T. Ishida, *Chem. Phys. Lett.* **2012**, *530*, 49-54.
- 38 G. Novitchi, W. Wernsdorfer, L. Chibotaru, J. P. Costes, C. E. Anson, A. K. Powell, *Angew. Chem. Int. Ed.* **2009**, *48*, 1614-1619.

Graphical Abstract



The Cu-Gd oximate bridge is responsible for the presence of an antiferromagnetic interaction in a trinuclear Cu-Gd-Cu complex, isostructural to the Cu-Tb-Cu one, contrary to what is observed in the magnetic behavior of phenoxo-bridged Cu-Gd complexes.

Graphical Abstract



The Cu-Gd oximato bridge, which is responsible for the presence of an antiferromagnetic interaction in a trinuclear Cu-Gd-Cu complex, isostructural to the Cu-Tb-Cu one, contrary to what is observed in the magnetic behavior of phenoxo-bridged Cu-Gd complexes.